

SIMULATION AND REALIZATION OF AN ACTIVE METAMATERIAL CELL FOR GSM/UMTS

M. Al-Azab

Department of Electronics and Communication
Higher Technological Institute
Ramadan Tenth, Egypt

Abstract—Simulation and realization of an active metamaterial cell are presented. This metamaterial cell has a power loss due to resistance in the coils. This paper presents a new nanometer negative resistance MOSFET (NR-MOSFET), which is used as a controllable negative resistance to compensate for the nanometer metamaterial losses. The negative resistance was about $-320\ \Omega$. A form of a lumped circuit model with active and passive resonance is presented. A negative real part of the refractive index exists in a band width from 1.11 GHz to 1.22 GHz. This model can be used as a core cell for mobile communication smart antenna.

1. INTRODUCTION

Metamaterial is known as an isotropic material with simultaneously negative permeability $\mu(\omega)$ and permittivity $\varepsilon(\omega)$, which may yield negative refraction. It is also known as left-hand material, due to the fact that the electric field, magnetic field, and the wave vector constitute a left-handed set of vectors [1–5]. Metamaterial does not exist naturally; however, it is possible to make an artificial left-handed material with negative $\mu(\omega)$ and $\varepsilon(\omega)$ in the same frequency range [6–8]. The sign of the refractive index depends on the location of zeros and poles of the $\mu(\omega) - \varepsilon(\omega)$ in the complex frequency plane. This indicates that it is possible to obtain negative refractive index without any magnetic resonance, $\mu = 1$, but instead two electric resonances [9, 10]. Artificial metamaterials often suffer from a limited performance due to large losses. There are many solutions to improve the performance, such as, to combine metamaterials with active gain, or create active metamaterials [11, 12]. Negative Resistance MOSFET (NR-MOSFET) was introduced for overcoming inherent losses in metamaterial.

The refractive index n is known as [13]:

$$n = \sqrt{\varepsilon(\omega)\mu(\omega)} \quad (1)$$

The sign of n must be identified to ensure the causality which means that the front of an electromagnetic wave can not travel faster than the vacuum velocity of light. When a plane wave is normally incident from vacuum to a semi-infinite medium the transmission S is given by the Fresnel equation [14]:

$$S = \frac{2\mu}{\mu + n} e^{j\omega nd/c} \quad (2)$$

where d is the distance between the excitation point and the observation point, c is the light velocity. If the excitation origin is $U(t)\cos(\omega_1 t)$, where $U(t)$ is the unit step function and ω_1 is the excitation frequency, the electric field in the metamaterial can be expressed as [15]:

$$E(d, t) = \frac{1}{2\pi} \int_{-\infty}^{\infty} \frac{\omega S e^{-j\omega t}}{\omega_1^2 - \omega^2} d\omega \quad (3)$$

where ω_1 is the excitation frequency to be $\omega_1 = 1.4\omega_0$, where ω_0 is the resonance frequency. If the frequency of the incident light lies within a spectral band slightly above the resonance frequency, the effective magnetic permeability will be negative. On the other hand, these cells act as electric dipoles whose electric response can lead to a negative permittivity. Passive metamaterials often suffer from limited performance due to large losses. It has therefore been suggested to combine them with active gain media, or even create active metamaterials as a method for overcoming inherent losses in metamaterials [15].

Section 2 illustrates a model of active metamaterial. NR-MOSFET and modeling is presented in Section 3, and simulation results are presented in Section 4. Conclusion of this work is given in Section 5.

2. A MODEL ACTIVE METAMATERIAL

A model of active metamaterial consists of passive and active resonance was designed. A negative index medium based on a periodically L-C loaded transmission line was presented, Where the model was described electromagnetically by an effective permittivity $\varepsilon\varepsilon_0$ [F/m] and an effective permeability $\mu\mu_0$ [H/m], where ε_0 and μ_0 are the vacuum permittivity and permeability. The periodicity remains less

than $(\lambda_0/30)$, where λ_0 is the vacuum wave length. The transmission line shown in Figure 1. and straight forward analysis will give:

$$\frac{dV}{dz} = -Iz \tag{4}$$

$$\frac{dI}{dy} = -Vy \tag{5}$$

where z is the series impedance per unit length and y is the shunt admittance per unit length, combining Equations (4) and (5), yields

$$\frac{d^2V}{dz^2} + \beta^2V = 0 \tag{6}$$

where β is the propagation constant. Mapping the voltage V to E_y and the current I to $-H_x$, equations can be written as field equations:

$$\frac{dE_y}{dz} = -j\omega\mu\mu_0H_x \tag{7}$$

$$\frac{dH_x}{dz} = -j\omega\varepsilon\varepsilon_0E_y \tag{8}$$

which yields the effective material parameters. The propagation constant satisfies:

$$\beta^2 = -zy = \frac{\omega^2}{C^2}\varepsilon(\omega)\mu(\omega) \tag{9}$$

It can easily be seen that interchanging the inductance and capacitance of a conventional transmission line leads to negative μ and ε ; thus it becomes left-handed. We will have the impedance where the permeability is a sum of one passive and one active resonance beside the admittance where the permittivity, also, becomes a sum of one passive and one active resonance. A model circuit is given in Figures 2(a) and 2(b), where k is the propagation constant of the interconnecting transmission line and d is the unit-cell dimension [10, 11].

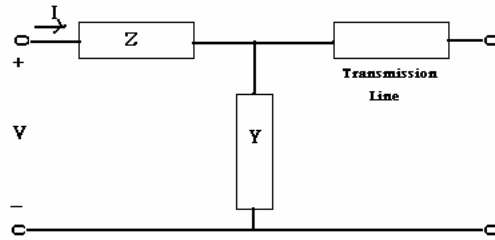


Figure 1. Conventional transmission line.

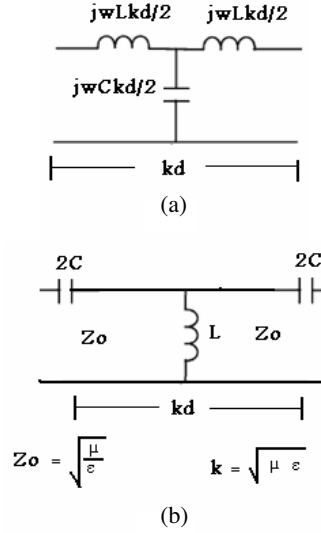


Figure 2. A realized dual transmission line cell.

A transmission line with additional impedance, admittance and negative resistance R_N is shown in Figure 3.

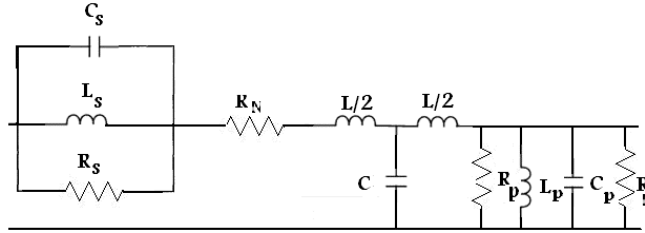


Figure 3. The proposed transmission line with additional impedance and admittance.

The total admittance is given by

$$Y = -j\omega C_p - \frac{1}{j\omega L_p} + \frac{R_N R_p}{R_N + R_p} \quad (10)$$

Combining Equations (9) and (10). We have

$$\varepsilon(\omega) = \frac{1}{\varepsilon_0 l} \left[C_p - \frac{1}{\omega^2 L_p} + \frac{R_N R_p}{j\omega(R_N + R_p)} \right] \quad (11)$$

The total impedance is given by

$$Z = -j\omega C_s - \frac{1}{j\omega L_s} + (R_s + R) \quad (12)$$

and

$$\mu(\omega) = \frac{1}{\mu_0 l} \left[C_s - \frac{1}{\omega^2 L_s} - \frac{(R_N + R_s)}{j\omega} \right] \quad (13)$$

where l is the length of the transmission line, C_s is the series capacitance and L_s is the series inductance, R_s is the series resistance and C_p , L_p and R_p are the parameters of passive resonator. R_N is the negative resistance device which provide gain.

3. NR-MOSFET THEORY AND MODELING

The idea and construction of the proposed voltage controlled NR-MOSFET is shown in Figure 4. It was realized using the poly silicon gate N-channel MOSFET technology. It consists of a MOSFET T_{NR} with channel length L_N , width Z_N and oxide thickeners h_{ON} , the channel width contraction is achieved using two additional P^+ lateral diffusions whose potential is maintained negative with respect to the channel well potential and its amplitude kept varying proportionally with the drain voltage V_{DS} . To carry out this requirements a MOSFET operational amplifier are designed so as to perform the desired amount of channel contraction. This operational amplifier is biased between $+V_R$ and $-V_R$ with V_R being the control voltage [17, 18].

A MOSFET operational amplifier was designed so as to reverse the polarity and has the desired amplitude needed to elaborate the wanted contraction and it was biased between the control voltages $+V_g$, $-V_g$. Since the channel well potential was always negative this design

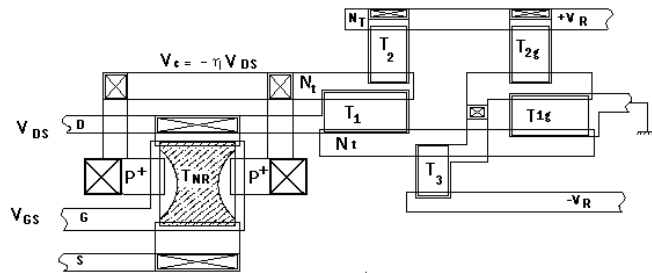


Figure 4. The construction of the proposed voltage controlled negative resistance.

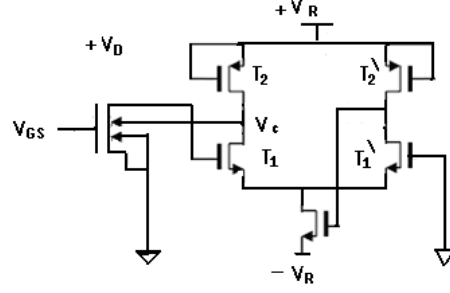


Figure 5. NR-MOSFET equivalent circuit.

guarantees a strong depletion of the N^+ version layer of the channel well. This leads to a depletion layer width W which increases steeply as V_{DS} increases, thus controlled decrease of the channel width and consequently channel current I_{DS} decreases as V_{DS} increases; we notice that the decrease of I_{DS} becomes more noticeable in the saturation region where I_{DS} should remain constant and cause more observable negative resistance behavior [13–15].

The variation of the channel width W and its dependence on the drain and gate voltages in saturation region will be approved. Referring to Figure 6. which shows the energy band diagram of the proposed negative resistance NR-MOSFET [19].

The variation of the potential V_Z with distance is given by:

$$V_Z = V_C + \frac{C_{ox}}{2d_o\epsilon_s} (V_{GS} - V_T - V_x) Z^2 \quad (14)$$

where V_C is the control voltage and is given by:

$$V_c = -\eta V_{DS}, \quad \eta = \frac{\sqrt{Z_1/L_1}}{\sqrt{Z_2/L_2}} \quad (15)$$

where Z_1 , Z_2 , L_1 , L_2 , are the channel width and length of the op-amp MOSFET T_1 and T_2 , d_o is the channel depth, C_{ox} is the oxide thickness, V_T is the threshold voltage and V_z is the channel potential at position X .

The amount of channel contraction may be calculated by equating the channel voltage to the surface potential, one can find:

$$W = \sqrt{\frac{2d_o\epsilon_s (V_s + \eta V_{DS})}{C_{ox} (V_{GS} - V_T - V_X)}} \quad (16)$$

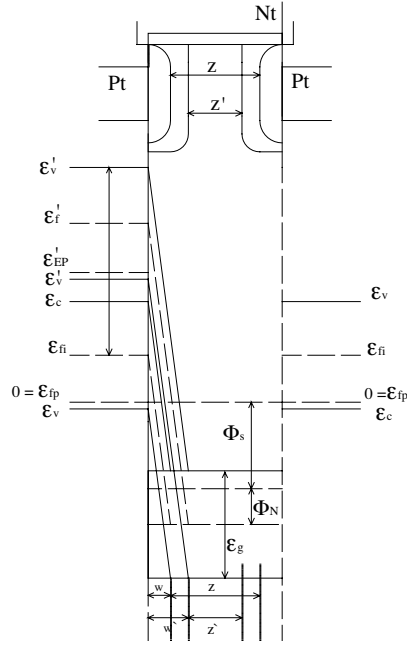


Figure 6. The energy band diagram for NR-MOSFET.

The effective channel width may be expressed in terms of position X in the channel from the source and the biasing voltages V_{DS} and V_{GS} as follows:

$$Z_{\text{efficient}} = Z - 2W \quad (17)$$

The modified drain current equation in the saturation region is therefore:

$$I_{DS} = \beta \frac{1}{2} \left[V_{GS} - V_T - V_{DS} \frac{X}{L} \right]^2 \quad (18)$$

where

$$\beta = \mu C_{ox} \frac{Z_{\text{effective}}}{L} \quad (19)$$

The Resistance equivalent

$$R_N = \frac{dV_{DS}}{dI_{DS}} \quad (20)$$

$$R_N = - \frac{L^2}{\mu C_{ox} (Z - 2W) \left(V_{GS} - V_T - V_{DS} \frac{X}{L} \right)} \quad (21)$$

This indicates that the NR-MOSFET acquire a negative resistance in saturation region of operation. Controlling the geometrical ratio of the NR MOSFET controls this resistance. To realize a nanogeometric NR-MOSFET, advanced fabrication process based on ion implantation will be used [18, 19]. We can see that as the negative resistance may be controlled by the frequency and the contraction of the channel width until we reach to the low loss of the metamaterials cell.

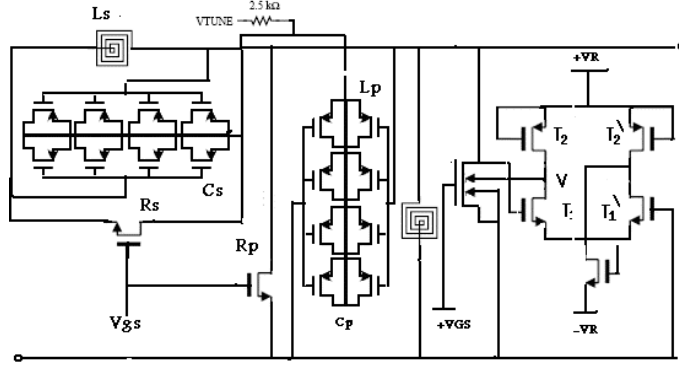


Figure 7. The proposed transmission line realization with spiral coil and MOS varactors and the NR-MOSFET.

4. SIMULATION RESULTS

Numerical simulation of the electric field for a proposed model with electric field versus distance and time for a causal excitation $[u(t) - u(t - 20 \text{ ns})] \cos(2\pi f_1 t)$, where $f_1 = 1.219 \text{ GHz}$, thickness = 150 times the length, length = 0.83 cm, at $t = 3.1 \text{ ns}$. Figure 7 shows the proposed transmission line with on chip spiral coil and MOS varactors and the NR-MOSFET. Figure 8 shows the dependence of the $I_{DS} - V_{DS}$ characteristics on the value of the parameter η and geometries. We observe that I_{DS} is still increasing proportionally in the ohmic region with V_{DS} but at smaller rate. Then I_{DS} begins to decrease as increasing V_{DS} in the saturation region. The rate of decreases becomes more important at greater values of η . This behavior is attributed to the increase of the depletion region width with V_{DS} . It becomes more noticeable of at greater values of V_{GS} . Figure 9 shows Refractive index versus frequency for the proposed Transmission-line. Electric field against distance and time is shown in Figure 10, for a causal excitation $[u(t) - u(t - 20 \text{ ns})] \cos(2\pi f_1 t)$; $f_1 = 1.23 \text{ GHz}$, $d = 150 \times 0.83 \text{ cm}$, $t = 3.1 \text{ ns}$.

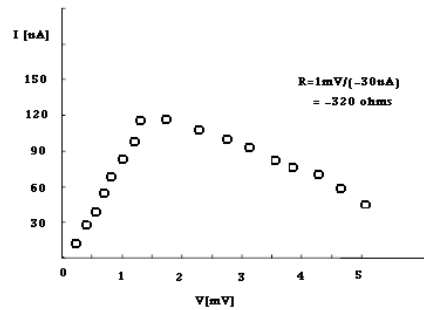


Figure 8. Current-voltage characteristics for NR-MOSFET.

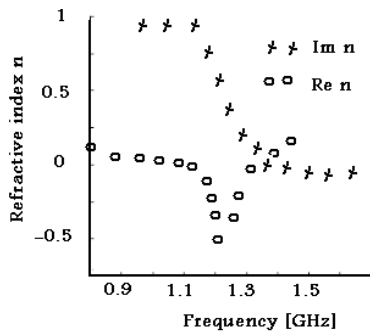


Figure 9. Refractive index versus frequency for the proposed Transmission-line.

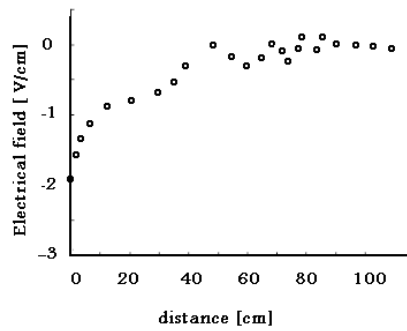


Figure 10. Electric field against distance and time.

5. CONCLUSION

This paper gives a simple analytical model for frequency dependent, voltage controlled, low loss metamaterial cell. The cell is composed of LC transmission line and a nanometer negative resistance NR-MOSFET. Although the cell always remains causal, the limitations like the Kramers-Kronig relation (for lossless particles) was eliminated in this design. We may finally conclude that the paper present a general approach to the design of an effective class of metamaterials. We hope that the model of this paper clearly demonstrate the power of the metamaterial concept that allows a great flexibility in the design and applications of nanotechnology and GSM/UMTS applications [16–20].

ACKNOWLEDGMENT

The author wish to thank Professor Adel ElHenawe, Head of Electronic Department, Ain Shams University, Cairo, Egypt, and the team of IC-Lab, for the opportunity to present these ideas and clarifying various points.

REFERENCES

1. Cui, T. J., H. F. Ma, R. Liu, B. Zhao, Q. Cheng, and J. Y. Chin, "A symmetrical circuit model describing all kinds of circuit meta materials," *Progress In Electromagnetics Research B*, Vol. 5, 63–76, 2008.
2. Lagarkov, A. N., V. N. Kisel, and V. N. Semenenko, "Wide-angle absorption by the use of a metamaterial plate," *Progress In Electromagnetics Research Letters*, Vol. 1, 35–44, 2008.
3. Abdalla, M. A. and Z. Hu, "On the study of left-handed coplanar waveguide coupler on ferrite substrate," *Progress In Electromagnetics Letters*, Vol. 1, 69–75, 2008.
4. Suyama, T., Y. Okuno, and T. Matsuda, "Plasmon resonance-absorption in a metal grating and its application for refractive-index measurement," *Journal of Electromagnetic Waves and Applications*, Vol. 20, No. 2, 185–169, 2006.
5. Grzegorezyk, T. M. and J. A. Kong, "Review of left-handed metamaterials: Evolution from theoretical and numerical studies to potential applications," *Journal of Electromagnetic Waves and Applications*, Vol. 20, No. 14, 2035–2064, 2006.
6. Ramakrishna, S. A. and J. B. Pendry, "Removal of absorption and increase in resolution in a near-field lens via optical gain," *Phys. Rev. B*, Vol. 67, No. 20, 201101, 2003.
7. Noginov, M. A., G. Zhu, M. Bahoura, J. Adegoke, C. E. Small, B. A. Ritzo, V. P. Drachev, and V. M. Shalaev, "Enhancement of surface plasmons in an Ag aggregate by optical gain in a dielectric medium," *Opt. Lett.*, Vol. 31, 3022, 2006.
8. Popov, A. K. and V. M. Shalaev, "Compensating losses in negative-index metamaterials by optical parametric amplification," *Opt. Lett.*, Vol. 31, 2169, 2006.
9. Shalaev, V. M., "Optical negative-index metamaterials," *Nat. Photonics*, Vol. 1, 41–48, 2007.
10. Chen, H., B.-I. Wu, and J. A. Kong, "Review of electromagnetic theory in left-handed materials," *Journal of Electromagnetic Waves and Applications*, Vol. 20, No. 15, 2137–2151, 2006.

11. Guo, Y. and R. Xu, "Ultra-wideband power splitting/combining technique using zero-degree left-handed transmission lines," *Journal of Electromagnetic Waves and Applications*, Vol. 21, No. 8, 1109–1118, 2007.
12. Wang, M. Y. and J. Xu, "FDTD study on scattering of metallic column covered by double-negative metamaterial," *Journal of Electromagnetic Waves and Applications*, Vol. 21, No. 14, 1905–1914, 2007.
13. Shelby, R. A., N. Smith, and S. Schultz, "Experimental verification of a negative index of refraction," *Science*, Vol. 229, 77–79, 2001.
14. Engheta, N., "An idea for thin sub wavelength cavity resonators using metamaterials with negative permittivity and permeability," *IEEE Antennas and Wireless Propagation Letters*, Vol. 1, No. 1, 10–13, 2002.
15. Abdalla, M., "ET alga differential 0.13 μm CMOS active inductor for high-frequency shifters," *IEEE ISCAS 2006*, 3341–3344, 2006.
16. Vainikainen P., et al., "Advances in diversity performance analysis of mobile terminal antennas," *International Symposium on Antennas and Propagation ISAP*, 649–652, Sendai, Japan, Aug. 2004.
17. El-Hennawy, A., E. Al-Mazuki, and S. A. L. Ghamdi, "Modeling and characterization of a new negative resistance NR-MOSFET for VLSI application. ICM 91," *Proc. the International Conference Micro. Electronics*, Cairo, Egypt, Dec. 1991.
18. Chua, L., J. Yu, and Y.-Y. Yu, "Bipolar-JFET-MOSFET negative resistance devices," *IEEE Transactions on Circuits and Systems*, Vol. 32, No. 1, 46–61, Jan. 1985.
19. Ramadan, A., A. El-Hennawe, K. Hassan, and A. A. Elnour, "Study and characterization of a new MOSFET voltage controlled negative resistance for super selective IC tank circuits," *International Journal of Electronics*, Vol. 86, No. 3, 311–319(9 ref.), 1999.
20. Ciaïis, P., R. Taraj, G. Kossiavas, and C. Luxey, "Design of an internal quad-band antenna for mobile phones," *IEEE Microwave and Wireless Components Letters*, Vol. 14, No. 4, 148–150, 2004.